Freezing phase scheme for complete-field characterization and coherent control of femtosecond optical pulses

J. Y. Huang*[1], M. C. Chen[1], C. L. Pan[1], and J. I. Chyi[2]
[1]*Department of Photonics and Institute of Electro-Optical Engineering, Chiao Tung University Hsinchu, Taiwan*
[2]*Department of Electrical Engineering, Central University Chung-Li, Taiwan*

jyhuang@cc.nctu.edu.tw,

Abstract

A freezing phase algorithm (FPA) has been developed and been applied to investigate three types of semiconductor saturable absorber Bragg reflectors. Our results reveal this new scheme to be faster, accurate and more immune to the noise and laser power fluctuation.

An attractive scheme to control and steer the quantum states of a complex system is adaptive laser pulses control[1)]. Several algorithms have been developed to tailor a coherent optical field for preparing specific products on the basis of fitness information. The concept appears to be universal and several progresses have already been reported[2-11)]. Recent study[5)] further indicates that the purpose of femtosecond coherent control study is not only able to control the evolution of a complex system but also to deduce the detailed dynamic mechanism from the optimal laser field used.

This paper reports a new scheme for adaptive coherent control with attractive features of fast and being immune to the noise and laser power fluctuation[12)]. Our method is useful for a variety of applications which require complete-field characterization and adaptive coherent control on the same setup.

To illustrate the freezing phase algorithm (FPA), a coherent optical field is first expressed in terms of its spectral components

$$E(t) = \sum_{n=0}^{N} A_n \exp\left[j(\omega_0 + 2\pi n \Delta\nu_F)t + \phi_n \right]. \qquad (1)$$

Here ω_0 is the optical carrier frequency, $\Delta\nu_F$ ϕ_n and A_n denote the frequency span, phase constant, and amplitude of the spectral components, respectively. In a typical 4-*f* pulse shaping apparatus, the pulse spectrum is angularly dispersed with a grating. We can impose a phase retardation pattern $\{\Phi_m\}$ on the M-pixel spatial light modulator (SLM) and transforms the input field into a shaped output. We arbitrarily choose pixel *j* from the SLM and use it as a modulation component by varying its phase retardance. The remaining M-1 pixels serve as the reference. The resulting peak intensity I_p of the shaped output pulse can be expressed as

$$I_p = |E_p|^2 = A_j^2 + B_j^2 + 2A_jB_j\cos(\theta_j - \vartheta_j). \qquad (2)$$

The first two terms represent the spectral intensities of the reference and the phase modulation component. The third term denotes interference between the two terms. By successively adjust every spectral component we can guide all components toward a "frozen phase state", where the shortest pulse can be produced.

To verify the function of FPA we first divide the 128-pixel SLM into two parts: the first group, which involves three neighboring pixels, plays the role of phase modulation. The other group, which contains the remaining 125 pixels, is used as the reference. The phase of the modulation group is then varied from 0 to 2π for maximizing the second-harmonic generation (SHG) intensity. The procedure is repeated by regrouping the SLM pixels until the phase retardations of all pixels are properly adjusted.

The experimentally measured SHG signal by an optical pulse reflected from a gold-coated mirror is shown in Fig. 1(a). For reference, the spectrum of the mode-locked laser pulse is also plotted along the y-axis to mark the corresponding wavelengths of the SLM pixels. The SHG modulation patterns yield information about the phase distortion of the optical pulse. The experimental result reported here also confirms the prediction of Eq. (2) that the SHG modulation sensitively depends on the amplitude of the spectral components chosen. Once the pixels lie outside the spectral range of the optical pulse, the SHG intensity modulation is no longer

observable.

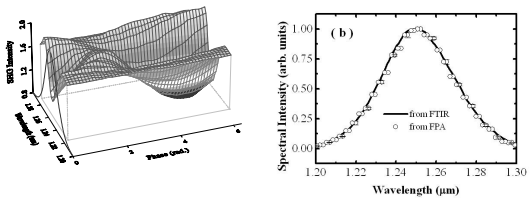

Fig. 1. (a) Measured SHG signal with an optical pulse reflected from a gold-coated mirror is plotted as a function of the phase retardation of the phase modulation group of three consecutive pixels and their corresponding wavelength in a 4-*f* pulse shaper apparatus. (b) Spectral-phase sensitivity plot of SHG deduced from freezing-phase algorithm (FPA, open circles) and the optical pulse spectrum measured with Fourier-transformed infrared spectroscopy (FTIR, solid line).

We further apply our adaptive control apparatus on three types of semiconductor Bragg reflectors (SBR). The first SBR device comprises of two coupled $Ga_{0.47}In_{0.53}As$ quantum wells which are embedded in an $Al_{0.48}In_{0.52}As$ quarter wave layer on a distributed Bragg reflector (DBR) stack (hereafter is abbreviated as *d*-QW). The other is self-assembled InAs quantum-dots layer embedded in a quarter-wave-thick (QD-λ/4) or half-wave-thick (QD-λ/2) GaAs layer on a DBR stack.

We used the SHG spectral-phase sensitivity (see Fig. 1(a)) to determine the spectral profile. Fig. 2(a) presents a direct comparison of the spectral profiles of optical pulse reflected from the *d*-QW sample deduced with FPA and that measured with FTIR. An excellent agreement was found. We then present the measured phase profiles with FPA for the three SBR devices in Fig. 2(b). The measured spectral phase profiles are similar to that obtained with SHG-FROG technique. Note that the device structure of QD-λ/2 is similar to QD-λ/4 except a twice thicker QD-embedded layer in QD-λ/2. The clearly distinguishable differences in the spectral phase profiles ensure that our new complete-field characterization scheme is sensitive and accurate enough to reveal influences on femtosecond optical pulse from subtle changes in SBR structures. Furthermore, unlike SHG-FROG where pulse characteristics are retrieved with sophisticated mathematical procedure, our method belongs to a direct approach.

A comparison of two-photon fluorescence (TPF) images of the InAs QD-λ/2 SBR was also made. A TPF image was taken with femtosecond laser pulses shaped by the phase pattern that yields the maximal TPF signal. Three times increase in the image contrast can be achieved with coherent control.

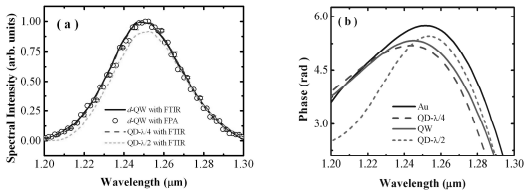

Fig. 2 (a) Spectral profiles of optical pulses reflected from *d*-QW (open circles) deduced with freezing-phase algorithm (FPA). For comparison, the pulse spectral profiles from *d*-QW (solid curve), QD-λ/4 (long dashed), and QD-λ/2 (short dashed) measured with Fourier-transformed infrared spectroscopy (FTIR) are also presented; (b) Spectral phase profiles of optical pulses reflected from Au-mirror (thin solid curve), *d*-QW (thick solid curve), InAs QD-λ/4 (long dashed), and InAs QD-λ/2 (short dashed) determined with FPA are shown.

Two sites in the scan region (labeled by P and S) are subjected to further study. We can use TPF signal from the P site or S site as the coherent control signal. Similar to the SHG study, we can also define the TPF spectral-phase sensitivity as the modulation depth of TPF signal when a spectral phase component of the excitation pulse is chosen to vary from 0 to 2π. The dotted and the dashed curves in Fig. 3 represent the spectral-phase sensitivity plot of TPF from the S and P sites, respectively. The spectral-phase sensitivity at the P site peaks at 1.25 μm, which is about 10 nm blue shift from that at the S-site. The corresponding P-site TPF spectrum was found to peak at 886 nm, while the S-site spectral peak locates at 868 nm. The 18-nm red-shift of the TPF spectrum at the P-site could originate from a localized strained GaAs structure with modified conduction band.

Note that the two phase patterns S' and S'_{SHG} that maximize TPF and SHG at the S-site are almost identical. The excited-state amplitude generated from two-photon excitation process serves as the common source of SHG and TPF. The two signals differ only on the emission process. SHG is a coherent process, while for TPF the emission is incoherent. The difference between SHG and TPF is very similar to the case of resonant Raman scattering and hot luminescence.

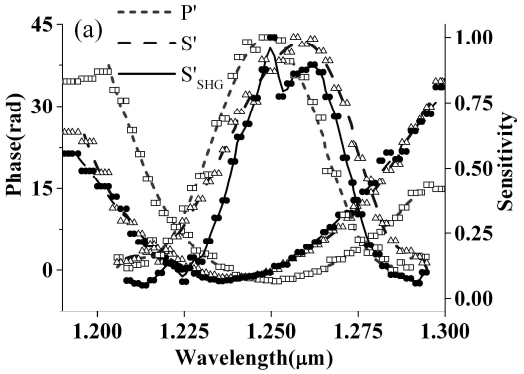

Fig. 3 Spectral-phase sensitivity curves of two-photon fluorescence (TPF) and the spectral-phase patterns used to yield maximum TPF signal from the position P (short dashed) and S dashed). The same data for SHG (solid curve) are also included for comparison.

In summary, we have developed a freezing phase algorithm for adaptive coherent control with a femtosecond pulse shaper. This freezing phase scheme had been employed for analyzing multiphoton processes in InAs quantum dot saturable Bragg reflector (SBR). Our results show that the function of InAs quantum dots can be revealed in the spectral-phase sensitivity plot of second harmonic signal. Coherent control study offers an additional degree of freedom for distinguishing coherent and incoherent nonlinear optical processes. Our results suggest the new freezing phase scheme to be useful for various applications which require complete-field characterization and coherent control on one setup.

Acknowledgements

We acknowledge the financial support from the National Science Council of the Republic of China under grant NSC 92-2112-M-009-014.

References

1) R. S. Judson and H. Rabitz, "Teaching lasers to control molecules", Phys. Rev. Lett. **68**, 1500-1503 (1992).

2) N. Dudovich, B. Orion, and Y. Silberberg, "Single-pulse coherently controlled nonlinear Raman spectroscopy and microscopy", Nature **418**, 512-515 (2002).

3) T. Brixner, N. H. Damrauer, P. Niklaus, and G. Gerber, "Photoselective adaptive femtosecond quantum control in the liquid phase", Nature **414**, 57-60 (2001).

4) Igor Pastirk, Johanna M. Dela Cruz, Katherine A. Walowicz, Vadim V. Lozovoy, and Marcos Dantus, "Selective two-photon microscopy with shaped femtosecond pulses", Opt. Express **11**, 1695- (2003).

5) C. Daniel, J. Full, L. González, C. Lupulescu, J. Manz, A. Merli, S. Vajda, and L. Wöste, "Deciphering the reaction dynamics underlying optical control laser fields", Science **299**, 536-539 (2003).

6) A. Assion, T. Baumert, M. Bergt, T. Brixner, B. Kiefer, V. Seyfried, M. Strehle, and G. Gerber, "Control of chemical reactions by feedback-optimized phase-shaped femtosecond laser pulses", Science **282**, 919-922 (1998).

7) W. S. Warren, H. Rabitz, and M. Dahleh, "Coherent control of quantum dynamics: the dream is alive", Science **259**, 1581-1589 (1993).

8) T. C. Weinacht, J. L. White, and P. H. Bucksbaum, "Toward strong field mode-selective chemistry", J. Phys. Chem. A **103**, 10166-10168 (1999)

9) R. J. Levis, G. M. Menkir, and H. Rabitz, "Selective bond dissociation and rearrangement with optimally tailored strong-field laser pulses", Science **292,** 709-713 (2001).

10) C. J. Bardeen, V. V. Yakovlev, K. R. Wilson, S. D. Carpenter, P. M. Weber, and W. S. Warren, "Feedback quantum control of molecular electronic population transfer", Chem. Phys. Lett. **280**, 151-158 (1997).

11) R. Mizoguchi, K. Onda, S. S. Kano, and A. Wada, "Thinning out in optimized pulse shaping method using genetic algorithm", Rev. Sci. Instrum. **74**, 2670-2674 (2003).

12) M. C. Chen, J. Y. Huang, Q. Yang, C. L. Pan and J. I. Chyi, J. Opt. Soc. Am. **B22**, 1 (May, 2005).